

Lecture 10, Nov, 11, 2015

The Kalman Filter (Polavarapu: Chapter 6.1-6.5)

Why we use a filter: “To obtain an ‘optimal’ estimate of a desired quantity from data provided by a noisy environment” [Maybeck, 1979]

The Kalman filter:

- “combines all available measurement data, plus prior knowledge about the system and measuring devices, to produce an estimate of the desired variables in such a manner that the error is minimized statistically” [Maybeck, 1979]
- “In a Bayesian context, it propagates the conditional probability density of the desired quantities, conditioned on knowledge of the actual data coming from the measuring devices” [Maybeck, 1979]

The Minimum Variance Estimator

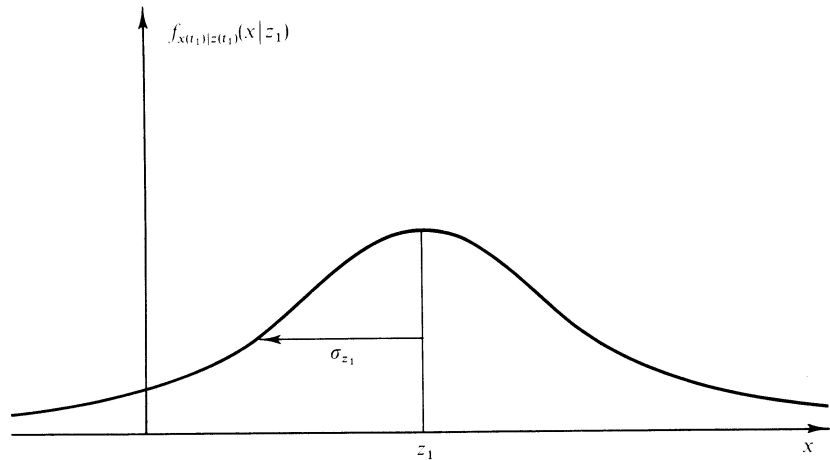


FIG. 1.4 Conditional density of position based on measured value z_1 .

$$\mu = z_1 + K(z_2 - z_1)$$

$$K = \frac{\sigma_1^2}{\sigma_1^2 + \sigma_2^2}$$

$$\sigma = \frac{\sigma_1^2 \sigma_2^2}{\sigma_1^2 + \sigma_2^2} = \frac{\sigma_2^2}{1 + \sigma_2^2 / \sigma_1^2} = \frac{\sigma_1^2}{\sigma_1^2 / \sigma_2^2 + 1}$$

Analysis error variance is always smaller than the a priori (background) and measurement variance

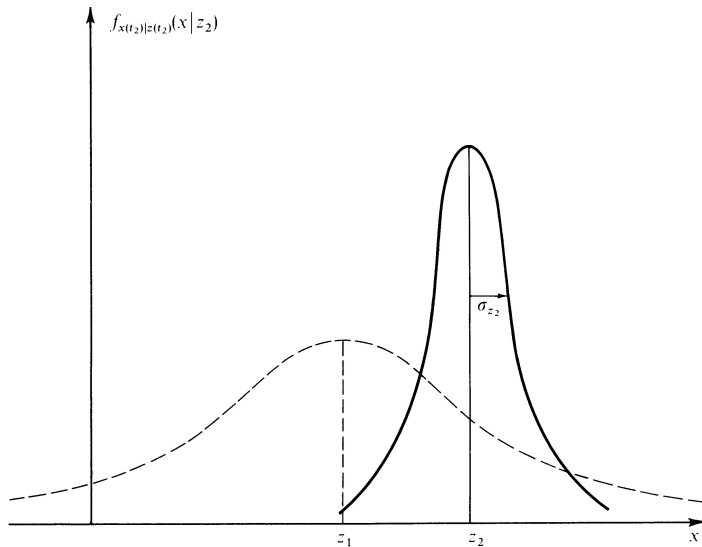


FIG. 1.5 Conditional density of position based on measurement z_2 alone.

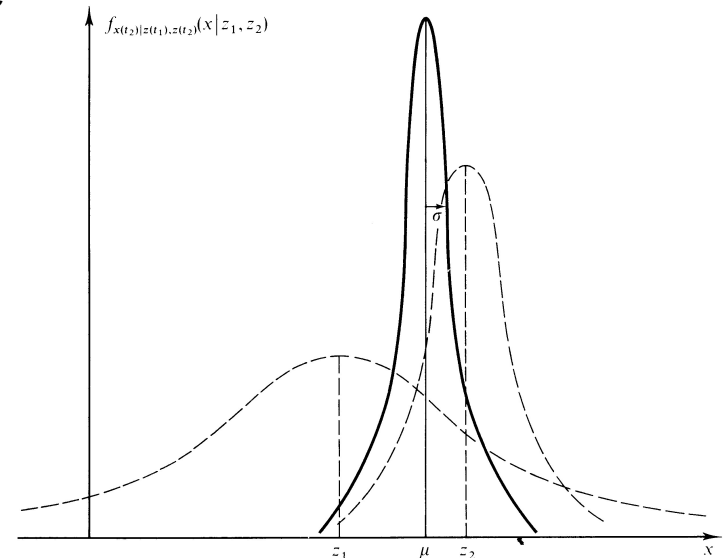


FIG. 1.6 Conditional density of position based on data z_1 and z_2 .

Propagation of the error covariance

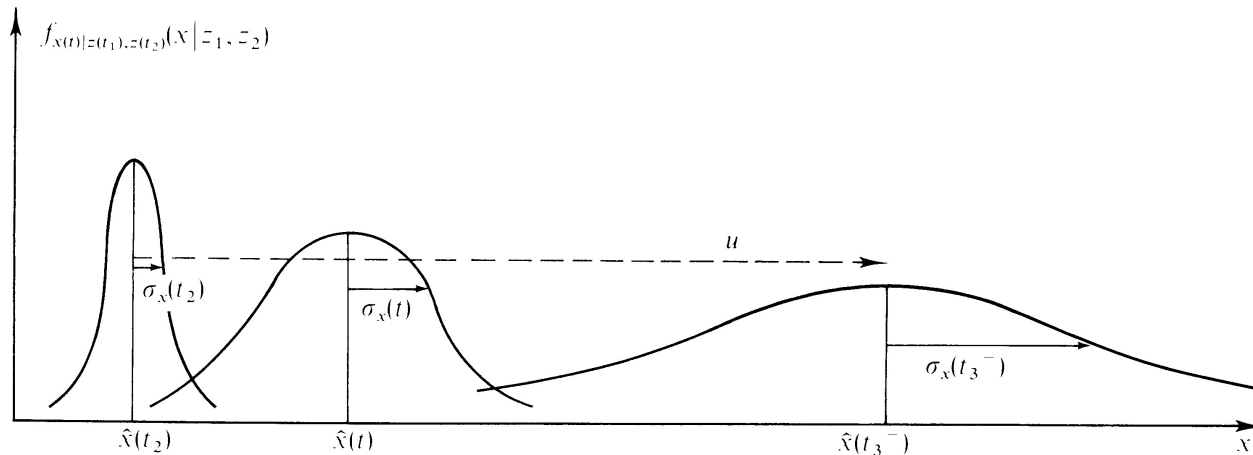


FIG. 1.7 Propagation of conditional probability density.

[Maybeck, 1979]

$$\frac{dx}{dt} = u + w$$

w = noise (model error)
 u = velocity

Derivation of the discrete linear Kalman Filter

Consider the following stochastic-dynamic system:

$$\begin{array}{l} n \times 1 \text{ state vector} \\ m \times 1 \text{ obs. vector} \end{array} \quad \begin{array}{l} \text{Model dynamics } n \times n \\ \mathbf{x}_{k+1} = \mathbf{M}_k \mathbf{x}_k + \mathbf{w}_k, \\ \mathbf{z}_k = \mathbf{H}_k \mathbf{x}_k + \mathbf{v}_k. \end{array} \quad \begin{array}{l} \text{Model error } n \times 1 \\ \text{Obs. Error } m \times 1 \\ = \text{instr.+rep. errors} \end{array} \quad (1)$$

Assumptions: for all k and l ,

$$\begin{array}{l} \text{Forward model} \\ m \times n \end{array} \quad \begin{array}{l} \langle \mathbf{w}_k \rangle = 0, \\ \langle \mathbf{v}_k \rangle = 0, \\ \langle \mathbf{w}_k (\mathbf{v}_l)^\top \rangle = 0. \end{array} \quad \begin{array}{l} \langle \mathbf{w}_k (\mathbf{w}_l)^\top \rangle = \mathbf{Q}_k \delta_l^k \\ \langle \mathbf{v}_k (\mathbf{v}_l)^\top \rangle = \mathbf{R}_k \delta_l^k \end{array} \quad (3)$$

These assumptions are not critical.

The KF problem is: given a prior estimate, $\hat{\mathbf{x}}_k^f$, what is the update or analysis, $\hat{\mathbf{x}}_k^a$, based on the measurements, \mathbf{z}_k ? Assume a linear, recursive form:

$$\hat{\mathbf{x}}_k^a = \tilde{\mathbf{L}}_k \hat{\mathbf{x}}_k^f + \tilde{\mathbf{K}}_k \mathbf{z}_k. \quad (4)$$

Initial conditions:

$$\langle \mathbf{x}_0 \rangle = \hat{\mathbf{x}}_0^f, \quad \mathbf{P}_0^f = \langle (\hat{\mathbf{x}}_0^f - \mathbf{x}_0)(\hat{\mathbf{x}}_0^f - \mathbf{x}_0)^\top \rangle.$$

This initial estimate is assumed uncorrelated with the model and observation errors for all time. The analysis and forecast errors are:

$$\begin{aligned} e_k^a &= \hat{\mathbf{x}}_k^a - \mathbf{x}_k \\ e_k^f &= \hat{\mathbf{x}}_k^f - \mathbf{x}_k. \end{aligned} \quad (5)$$

Subtract the truth from both sides of (4):

$$\begin{aligned} e_k^a &= \tilde{\mathbf{L}}_k(\hat{\mathbf{x}}_k^f + \mathbf{x}_k - \mathbf{x}_k) - \mathbf{x}_k + \tilde{\mathbf{K}}_k \mathbf{z}_k \\ &= \tilde{\mathbf{L}}_k e_k^f + \tilde{\mathbf{L}}_k \mathbf{x}_k - \mathbf{x}_k + \tilde{\mathbf{K}}_k (\mathbf{H}_k \mathbf{x}_k + \mathbf{v}_k) \\ &= (\tilde{\mathbf{L}}_k + \tilde{\mathbf{K}}_k \mathbf{H}_k - \mathbf{I}) \mathbf{x}_k + \tilde{\mathbf{L}}_k e_k^f + \tilde{\mathbf{K}}_k \mathbf{v}_k. \end{aligned} \quad (6)$$

Since

$$\langle e_k^a \rangle = (\tilde{\mathbf{L}}_k + \tilde{\mathbf{K}}_k \mathbf{H}_k - \mathbf{I}) \langle \mathbf{x}_k \rangle, \quad (7)$$

if we want an unbiased estimate, then

$$\tilde{\mathbf{L}}_k = \mathbf{I} - \tilde{\mathbf{K}}_k \mathbf{H}_k \quad (8)$$

so that the estimator (4) becomes

$$\hat{\mathbf{x}}_k^a = \hat{\mathbf{x}}_k^f + \tilde{\mathbf{K}}_k (\mathbf{z}_k - \mathbf{H}_k \hat{\mathbf{x}}_k^f). \quad (9)$$

and the estimation error is

$$e_k^a = (\mathbf{I} - \tilde{\mathbf{K}}_k \mathbf{H}_k) e_k^f + \tilde{\mathbf{K}}_k \mathbf{v}_k. \quad (10)$$

$\tilde{\mathbf{K}}_k$ is the weight given to observations.

$$\begin{aligned}
\mathbf{P}_k^a &= \langle (\mathbf{e}_k^a)(\mathbf{e}_k^a)^\top \rangle \\
&= (\mathbf{I} - \tilde{\mathbf{K}}_k \mathbf{H}_k) \mathbf{P}_k^f (\mathbf{I} - \tilde{\mathbf{K}}_k \mathbf{H}_k)^\top + \tilde{\mathbf{K}}_k \mathbf{R}_k \tilde{\mathbf{K}}_k^\top
\end{aligned} \tag{11}$$

To update the estimate, we use our forecast model:

$$\hat{\mathbf{x}}_{k+1}^f = \mathbf{M}_k \hat{\mathbf{x}}_k^a. \tag{12}$$

Thus we can subtract the true evolution (12) - (1) to get the forecast error:

$$\mathbf{e}_{k+1}^f = \mathbf{M}_k \mathbf{e}_k^a - \mathbf{w}_k. \tag{13}$$

If the analysis is unbiased, then the forecast is unbiased since our model error was assumed to be unbiased. The forecast error covariance is by definition,

$$\begin{aligned}
\mathbf{P}_{k+1}^f &= \langle (\mathbf{e}_{k+1}^f)(\mathbf{e}_{k+1}^f)^\top \rangle \\
&= \langle (\mathbf{M}_k \mathbf{e}_k^a - \mathbf{w}_k)(\mathbf{M}_k \mathbf{e}_k^a - \mathbf{w}_k)^\top \rangle \\
&= \mathbf{M}_k \langle (\mathbf{e}_k^a)(\mathbf{e}_k^a)^\top \rangle \mathbf{M}_k^\top + \langle (\mathbf{w}_k)(\mathbf{w}_k)^\top \rangle \\
\text{predictability error} &\rightarrow \underline{\mathbf{M}_k \mathbf{P}_k^a \mathbf{M}_k^\top} + \mathbf{Q}_k.
\end{aligned} \tag{14}$$

Proof that analysis and obs errors are uncorrelated at all times is by induction using the fact that the initial state and model errors are uncorrelated.

Note that \mathbf{P}^a and \mathbf{P}^f are independent of obs, background and analyses.

The Kalman Filter algorithm

Enter initial guess

$$\hat{\mathbf{x}}_0^f, \mathbf{P}_0^f$$

Compute Kalman Gain

$$\mathbf{K}_k = \mathbf{P}_k^f \mathbf{H}_k^T (\mathbf{H}_k \mathbf{P}_k^f \mathbf{H}_k + \mathbf{R}_k)^{-1}$$

forecast step:

$$\hat{\mathbf{x}}_{k+1}^f = \mathbf{M}_k \hat{\mathbf{x}}_k^a$$

$$\mathbf{P}_{k+1}^f = \mathbf{M}_k \mathbf{P}_k^a \mathbf{M}_k^T + \mathbf{Q}_k$$

Update estimate with obs.

$$\hat{\mathbf{x}}_k^a = \hat{\mathbf{x}}_k^f + \mathbf{K}_k (\mathbf{z}_k - \mathbf{H}_k \hat{\mathbf{x}}_k^f)$$

Compute analysis error cov.

$$\mathbf{P}_k^a = (\mathbf{I} - \mathbf{K}_k \mathbf{H}_k) \mathbf{P}_k^f$$

\mathbf{z}_k

\mathbf{x}_k^a

The Extended Kalman Filter

Stochastic-dynamic system:

$$\begin{aligned}\mathbf{x}_{k+1} &= M_k(\mathbf{x}_k) + \mathbf{e}_k^q \\ \mathbf{z}_k &= H_k(\mathbf{x}_k) + \mathbf{e}_k^r\end{aligned}$$

Nonlinear model and obs operator

$$\begin{aligned}M_k(\bar{\mathbf{x}} + \delta\mathbf{x}) &\approx M_k(\bar{\mathbf{x}}) + \frac{\partial M_k(\bar{\mathbf{x}})}{\partial \mathbf{x}} \delta\mathbf{x} \\ H_k(\bar{\mathbf{x}} + \delta\mathbf{x}) &\approx H_k(\bar{\mathbf{x}}) + \frac{\partial H_k(\bar{\mathbf{x}})}{\partial \mathbf{x}} \delta\mathbf{x}\end{aligned}$$

$$\frac{\partial M_k(\bar{\mathbf{x}})}{\partial \mathbf{x}} = \mathbf{M}_k, \quad \frac{\partial H_k(\bar{\mathbf{x}})}{\partial \mathbf{x}} = \mathbf{H}_k$$

Analysis step:

$$\begin{aligned}\mathbf{x}_k^a &= \mathbf{x}_k^f + \mathbf{K}_k(\mathbf{z}_k - H_k(\mathbf{x}_k^f)) \\ \mathbf{K}_k^\top &= \mathbf{P}_k^f \mathbf{H}_k^\top (\mathbf{H}_k \mathbf{P}_k^f \mathbf{H}_k^\top + \mathbf{R}_k)^{-1} \\ \mathbf{P}_k^a &= (\mathbf{I} - \mathbf{K}_k \mathbf{H}_k) \mathbf{P}_k^f\end{aligned}$$

Forecast step:

$$\begin{aligned}\mathbf{x}_{k+1}^f &= M_k(\mathbf{x}_k^a) \\ \mathbf{P}_{k+1}^f &= \mathbf{M}_k \mathbf{P}_k^a \mathbf{M}_k^\top + \mathbf{Q}_k\end{aligned}$$

with $\mathbf{x}_0^a = \mathbf{x}_0$ and $\mathbf{P}_0^a = \mathbf{P}_0$.

Summary of discrete Kalman filter equations

system model:

$$\mathbf{x}_{k+1} = \mathbf{M}_k \mathbf{x}_k + \mathbf{w}_k, \langle \mathbf{w}_k \rangle = 0, \langle \mathbf{w}_k (\mathbf{w}_l)^\top \rangle = \mathbf{Q}_k \delta_l^k$$

measurement model:

$$\mathbf{z}_k = \mathbf{H}_k \mathbf{x}_k + \mathbf{v}_k, \langle \mathbf{v}_k \rangle = 0, \langle \mathbf{v}_k (\mathbf{v}_l)^\top \rangle = \mathbf{R}_k \delta_l^k$$

other assumptions:

$$\langle \mathbf{w}_k (\mathbf{v}_l)^\top \rangle = 0$$

initial conditions: $\langle \mathbf{x}_0 \rangle = \hat{\mathbf{x}}_0^f, \mathbf{P}_0^f = \langle (\hat{\mathbf{x}}_0^f - \mathbf{x}_0) (\hat{\mathbf{x}}_0^f - \mathbf{x}_0)^\top \rangle$

forecast step:

$$\hat{\mathbf{x}}_{k+1}^f = \mathbf{M}_k \hat{\mathbf{x}}_k^a$$

$$\mathbf{P}_{k+1}^f = \mathbf{M}_k \mathbf{P}_k^a \mathbf{M}_k^\top + \mathbf{Q}_k$$

analysis step:

$$\hat{\mathbf{x}}_k^a = \hat{\mathbf{x}}_k^f + \mathbf{K}_k (\mathbf{z}_k - \mathbf{H}_k \hat{\mathbf{x}}_k^f)$$

$$\mathbf{P}_k^a = (\mathbf{I} - \mathbf{K}_k \mathbf{H}_k) \mathbf{P}_k^f$$

Kalman gain:

$$\mathbf{K}_k = \mathbf{P}_k^f \mathbf{H}_k^\top (\mathbf{H}_k \mathbf{P}_k^f \mathbf{H}_k + \mathbf{R}_k)^{-1}$$

Assimilation of Simulated Wind Lidar Data with a Kalman Filter

PIERRE GAUTHIER,* PHILIPPE COURTIER, AND PATRICK MOLL

CNRM, Météo-France, Paris, France

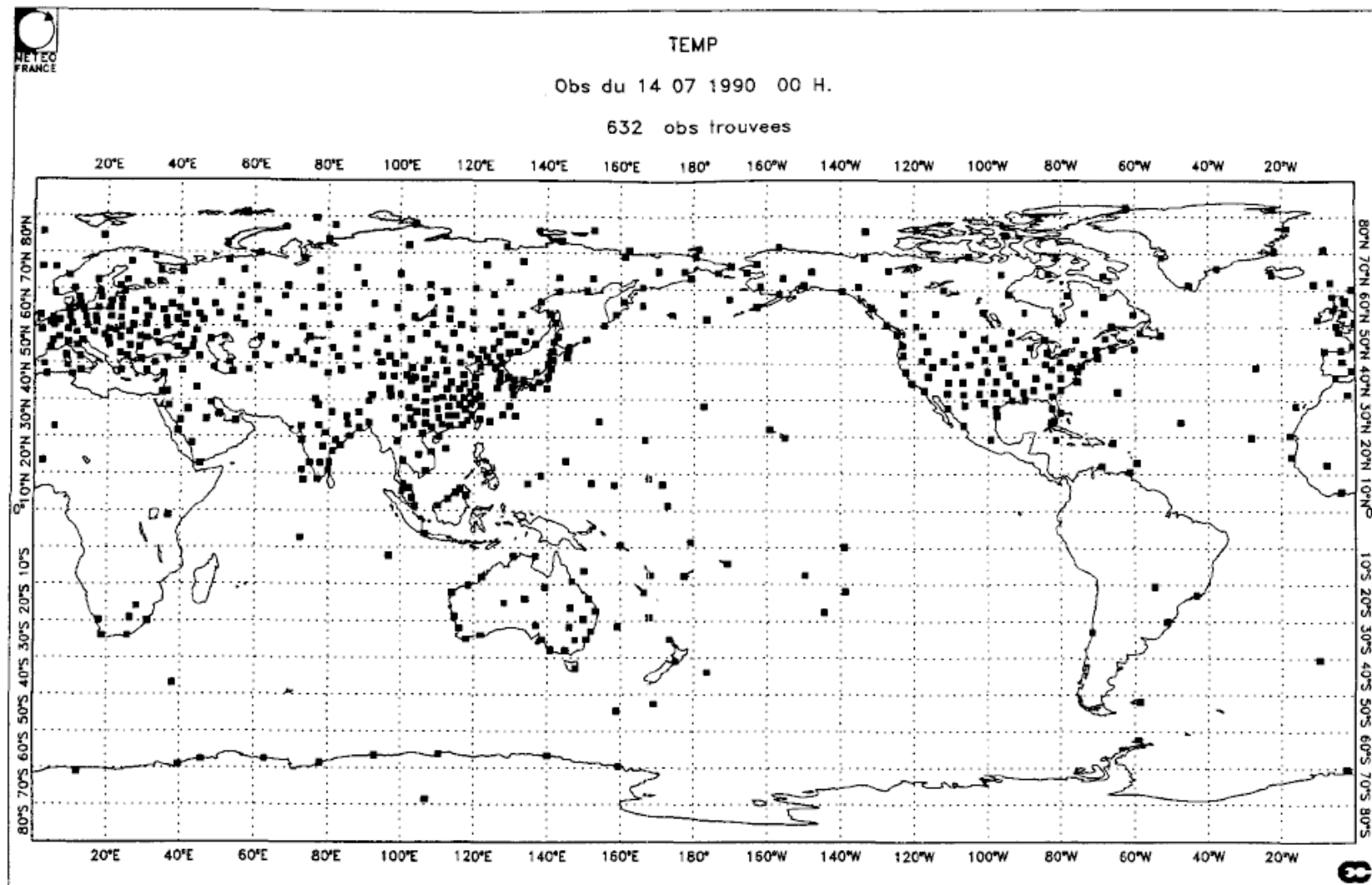
(Manuscript received 12 May 1992, in final form 30 November 1992)

ABSTRACT

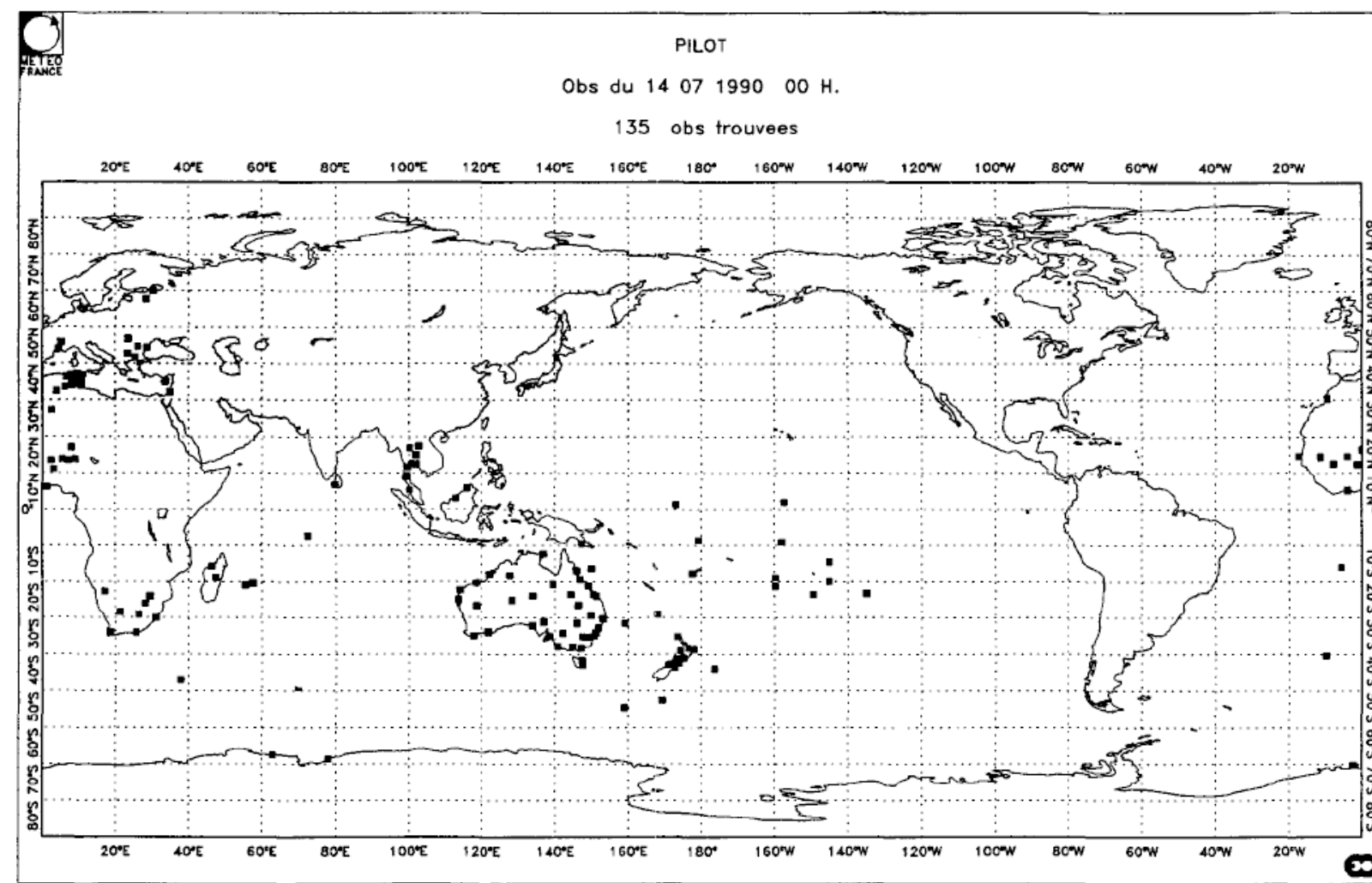
The object of this paper is to present some results obtained with an extended Kalman filter (EKF). First, a discussion is given of the way that the EKF has been implemented and tested for a global nondivergent barotropic model spectrally truncated at T21. In the present paper, the assimilation experiments focused solely on the time evolution of the forecast error covariances that are influenced by two factors: 1) their time integration performed here with the tangent linear model obtained from a linearization around the true trajectory and 2) the accuracy and distribution of the observations. Data from a simulated radiosonde network have been assimilated over a 24-h period. The results show that even though no model error has been considered, there can be a substantial forecast error growth, especially in regions where the flow is unstable and no data are available. The error growth is attributed to instability processes that are embedded within the complex flow configuration around which the nonlinear model is linearized to obtain the tangent linear model. The impact of different initial conditions for the forecast error covariance is also looked at. In an experiment where the time integration of the forecast error covariance is suppressed, the results show that error growth is suppressed, causing the analysis error variance to differ substantially from the variance field obtained with the EKF. Especially in regions where instability is present and no data are available, this "improved" optimal interpolation considers the forecast to be more accurate than it actually is.

In a second set of experiments, a mini-observing system simulation experiment has been conducted for which wind data from a proposed satellite-based lidar instrument have been simulated and added to the radiosonde data of the previous experiments. Two configurations of the instrument have been considered where the satellite is set on a polar orbit, at an altitude of 400 km in the first scenario and 800 km in the second. Compared to the results obtained with the radiosonde data alone, the global data coverage leads to an improvement in the analysis, especially in the Southern Hemisphere. Data being available in the regions of instability, the assimilation is now capable of putting a stop to the unlimited error growth observed in the previous experiments. Due to a degradation of the measurement when the instrument is at an altitude of 800 km, the analysis is more accurate for the 400-km case, but the low-altitude orbit (400 km) leaves holes in the tropical belt that the data assimilation scheme is not quite able to compensate for.

[Monthly Weather Review, 121, 1803-1820, 1993]



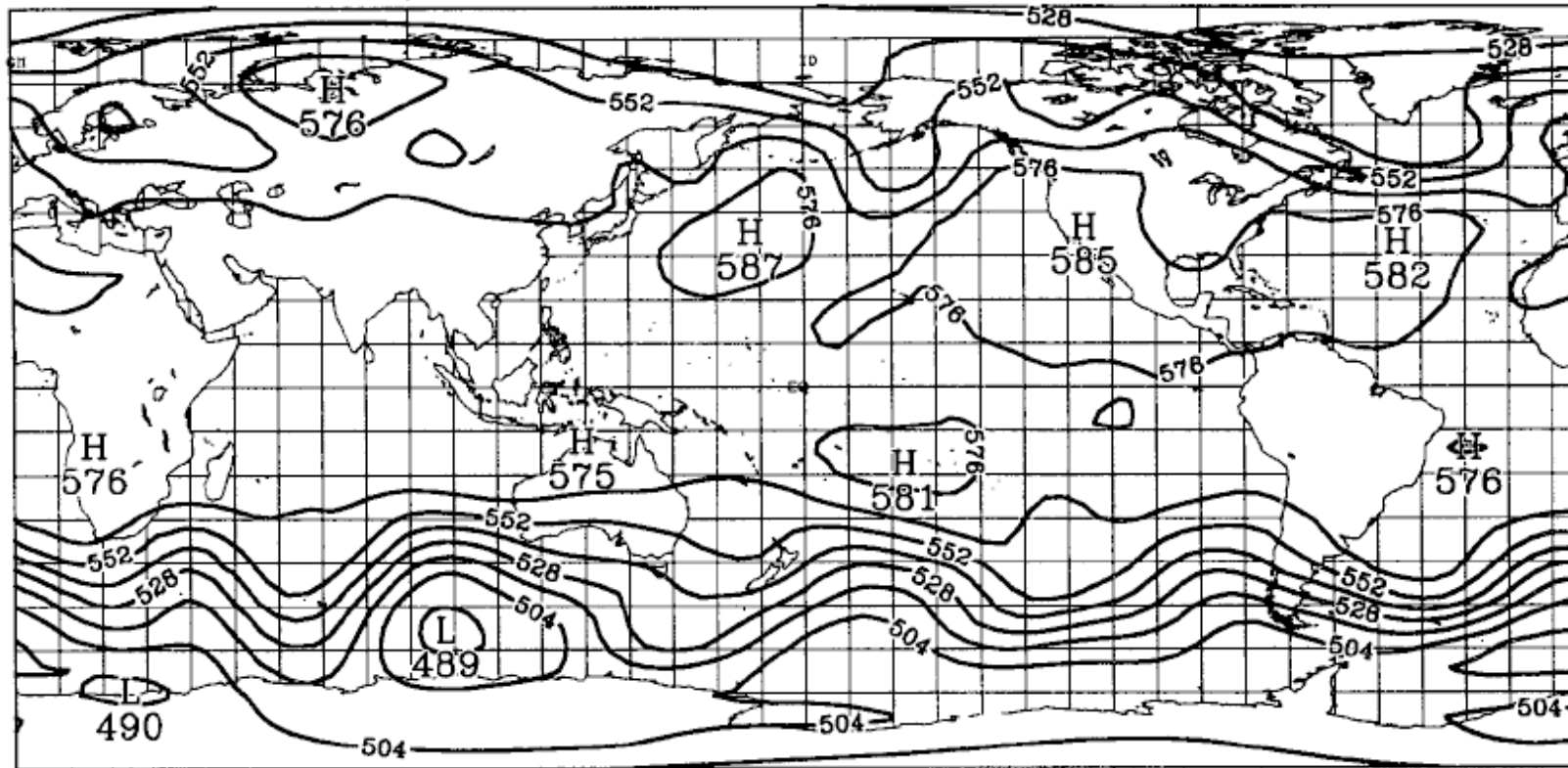
In situ observations used in OSSE



Gauthier et al (1993)

FIG. 1. Typical radiosonde network at 0000 UTC for TEMP and PILOT. This network is assumed to be the same every 6 h.

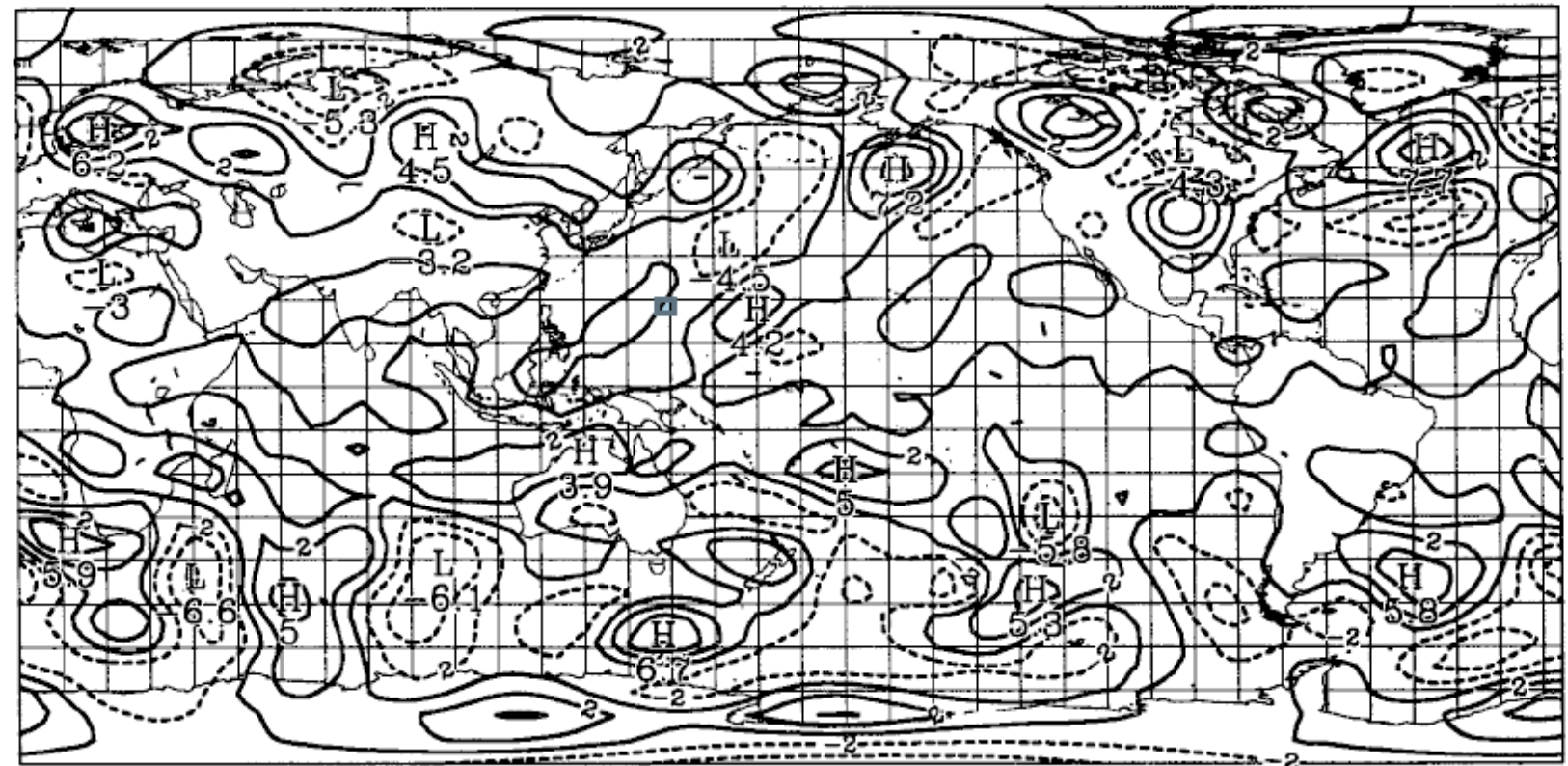
A) GEOPOTENTIAL HEIGHT (500 MB)



T = 0 (HRS)

Initial Conditions: Geopotential height and vorticity

B) VORTICITY (500 MB)

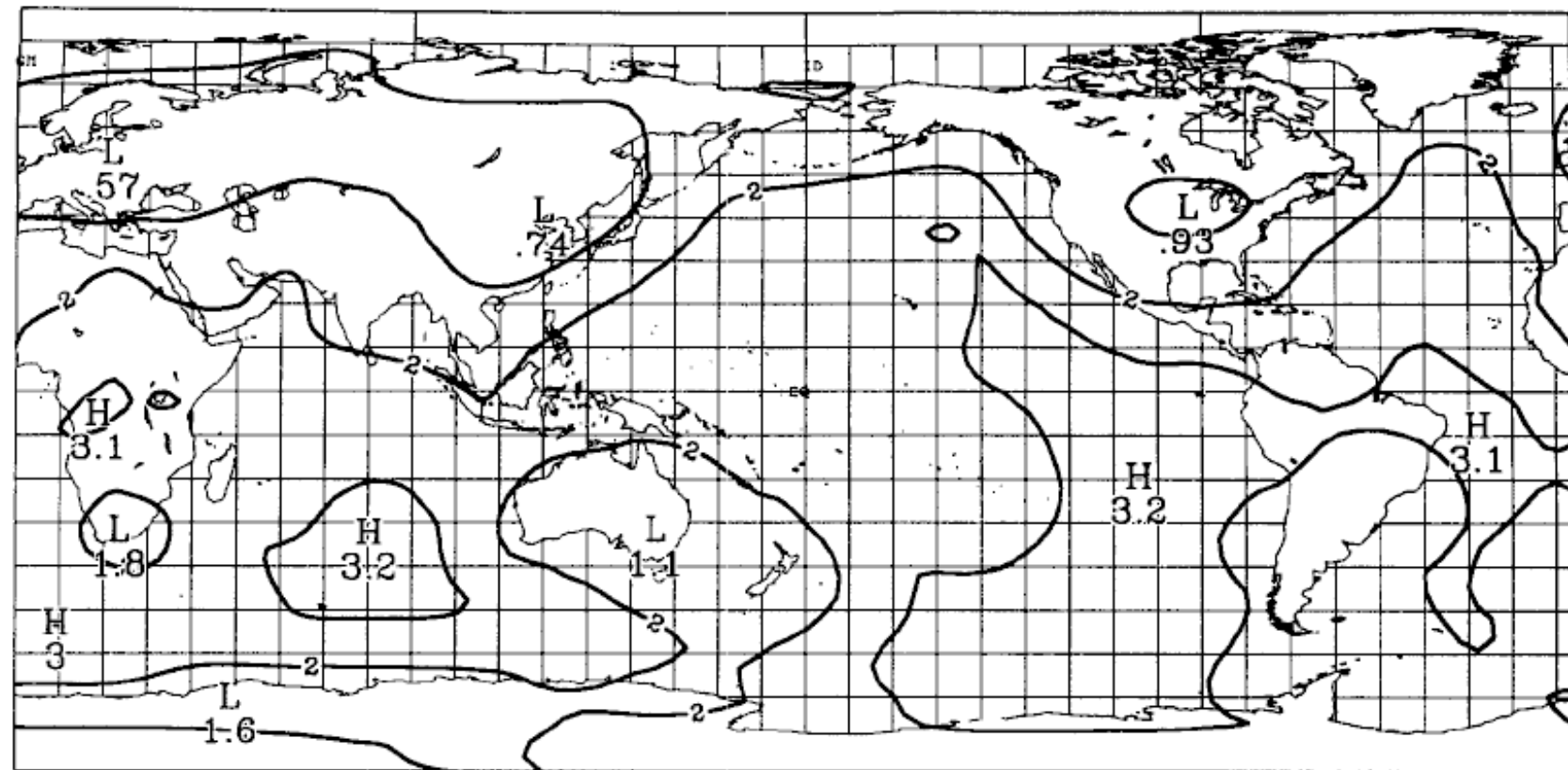


T = 0 (HRS)

Gauthier et al (1993)

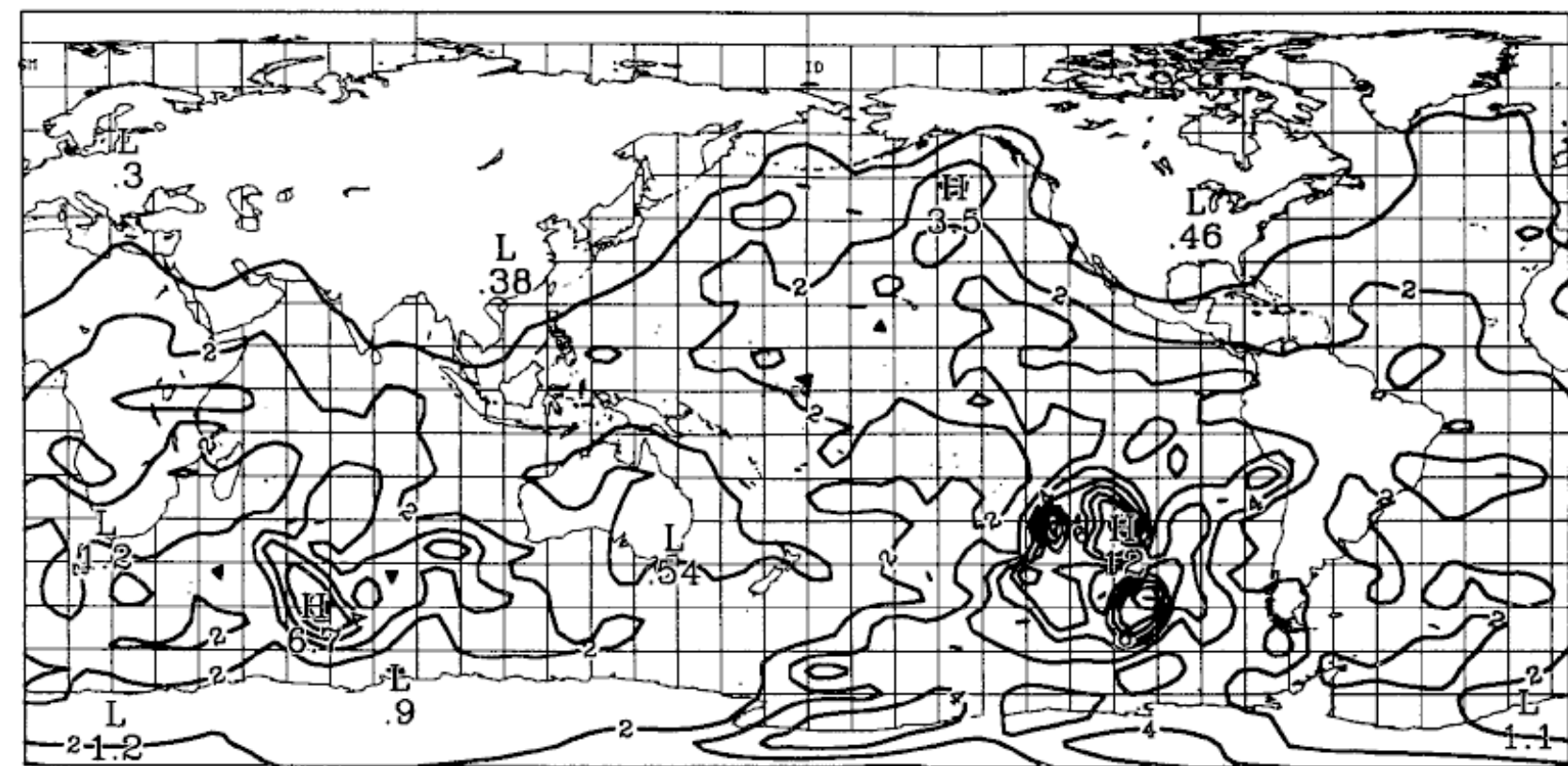
FIG. 2. Initial conditions on 14 July 1990: (a) geopotential field and (b) vorticity field.

-A-



T = 0 (HRS)

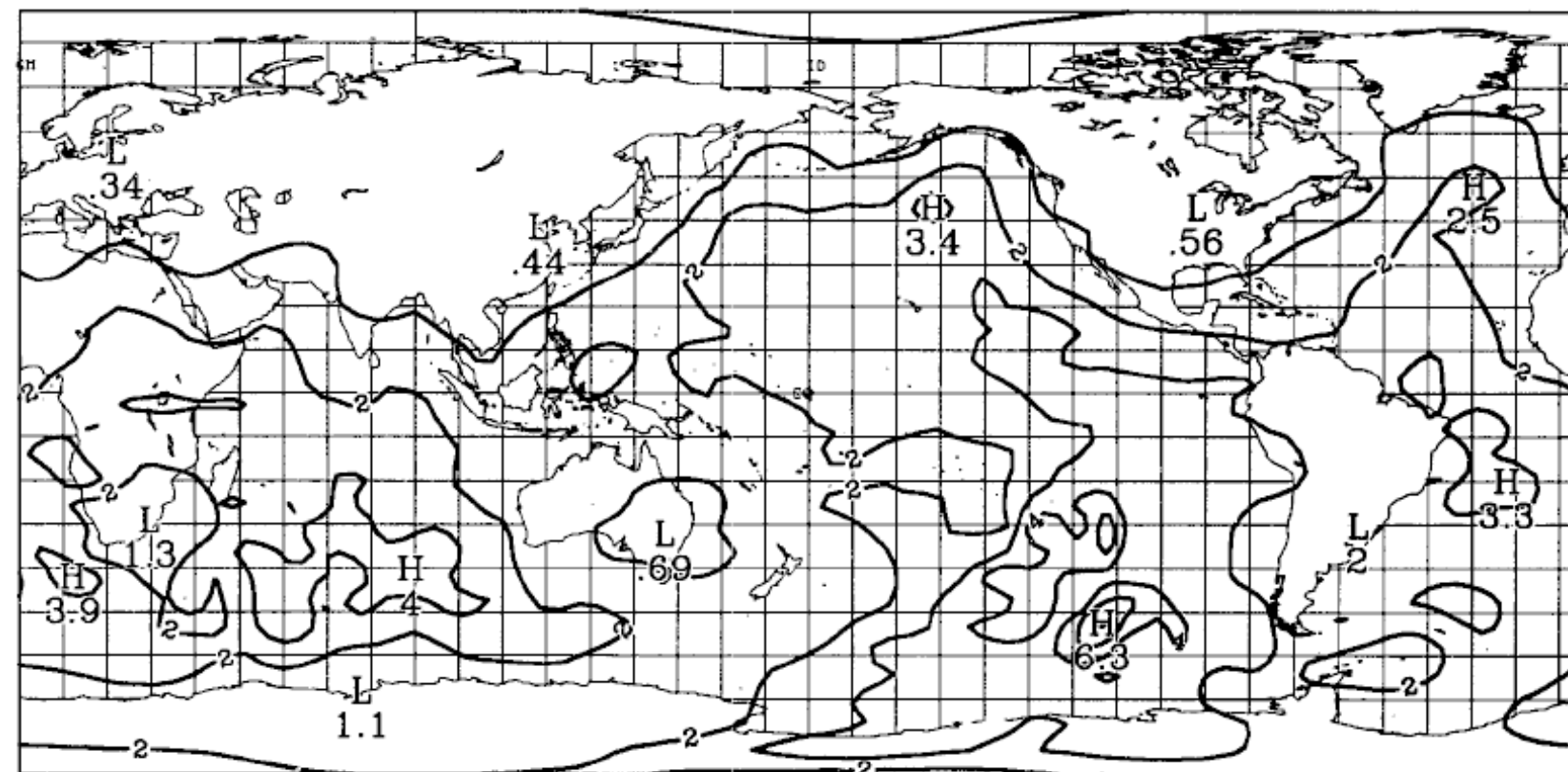
-C-



T = 24 (HRS)

Analysis error

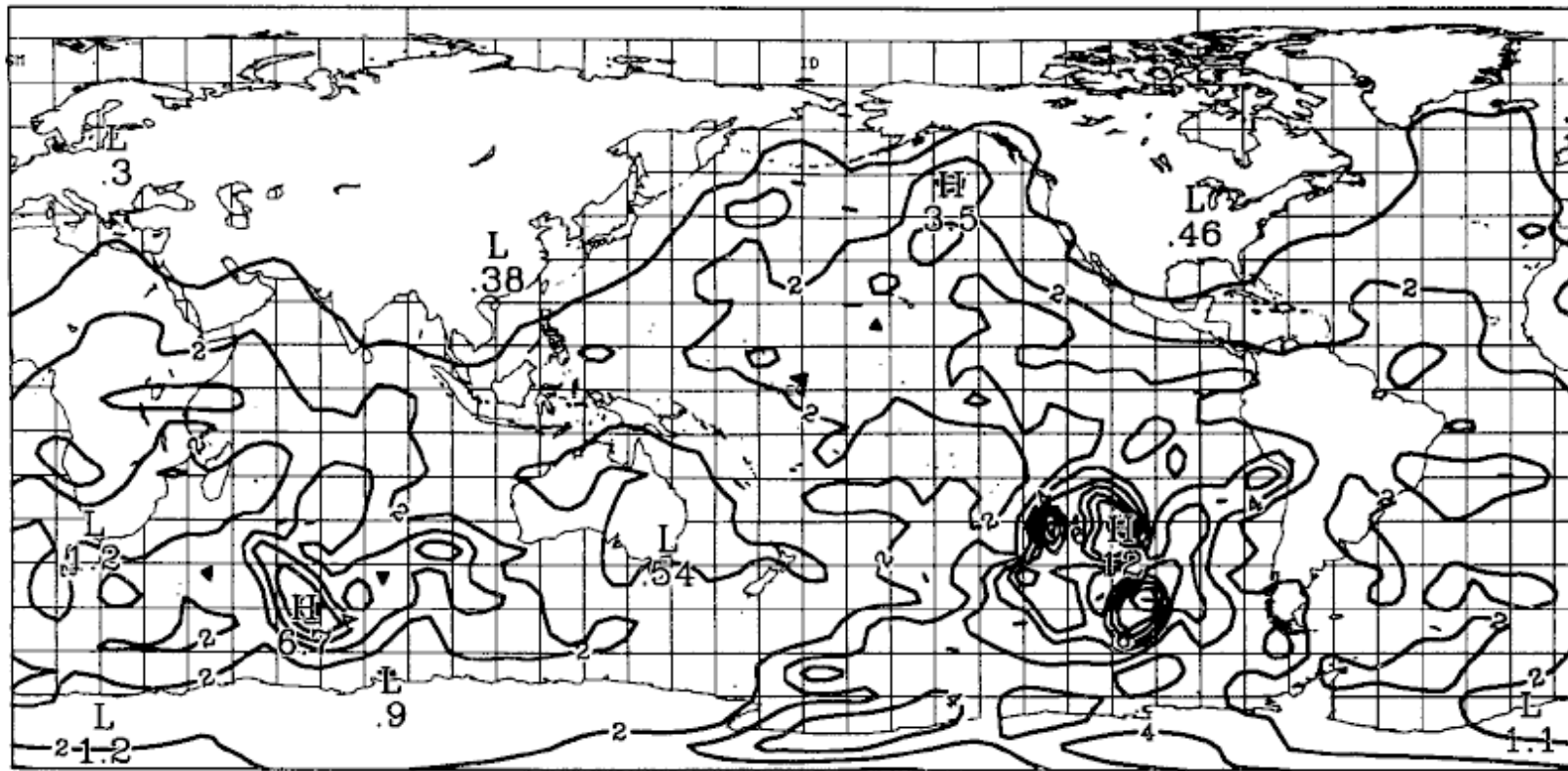
-B-



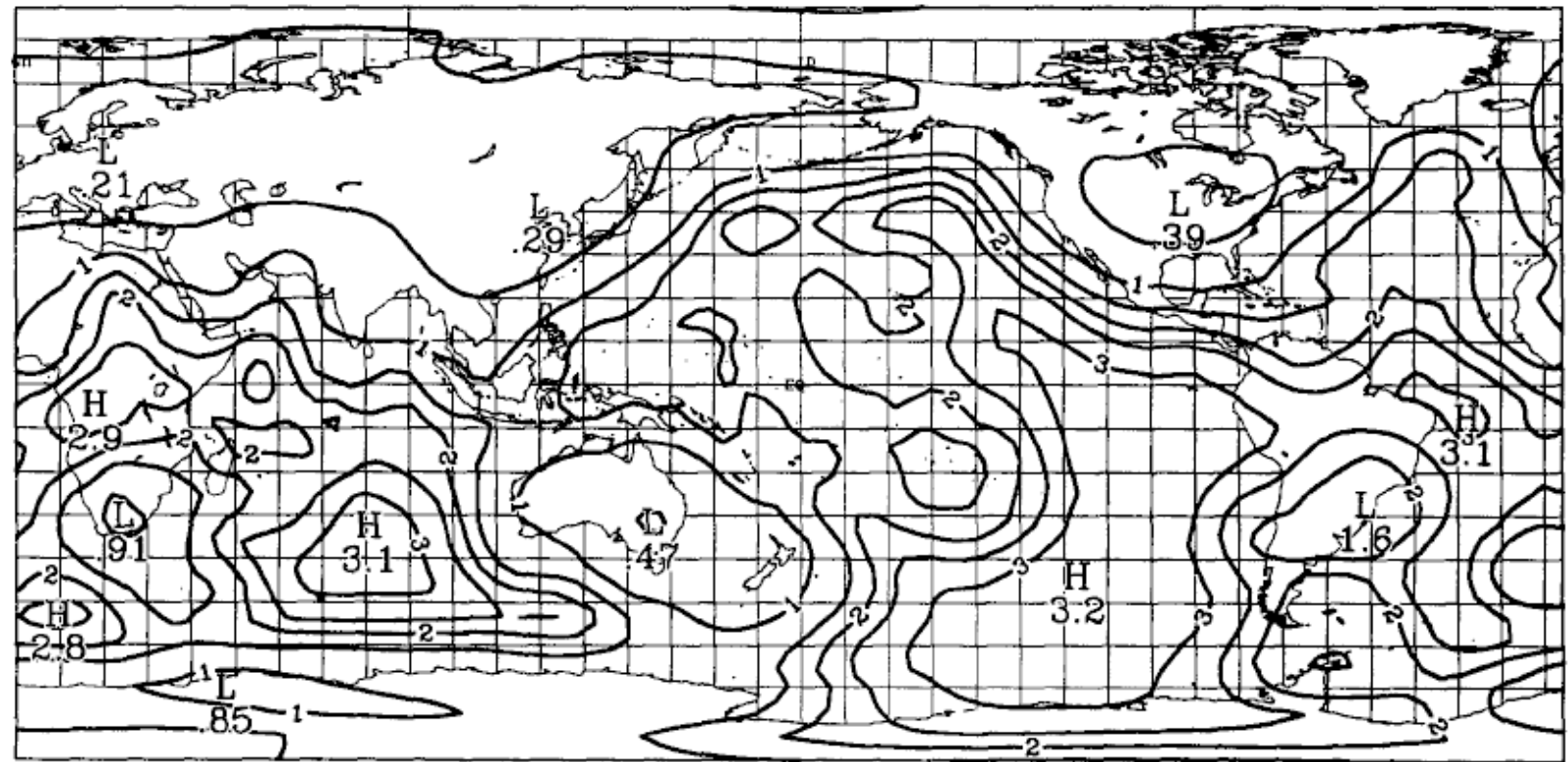
T = 12 (HRS)

FIG. 3. Analysis error variance resulting from an assimilation with the extended Kalman filter: (a) $t = 0$ h, (b) 12 h, and (c) 24 h. Units used are $1 \times 10^{-12} \text{ s}^{-2}$, with contour levels of 1 unit, and the characteristic length of the first-guess error is 1200 km.

Analysis error



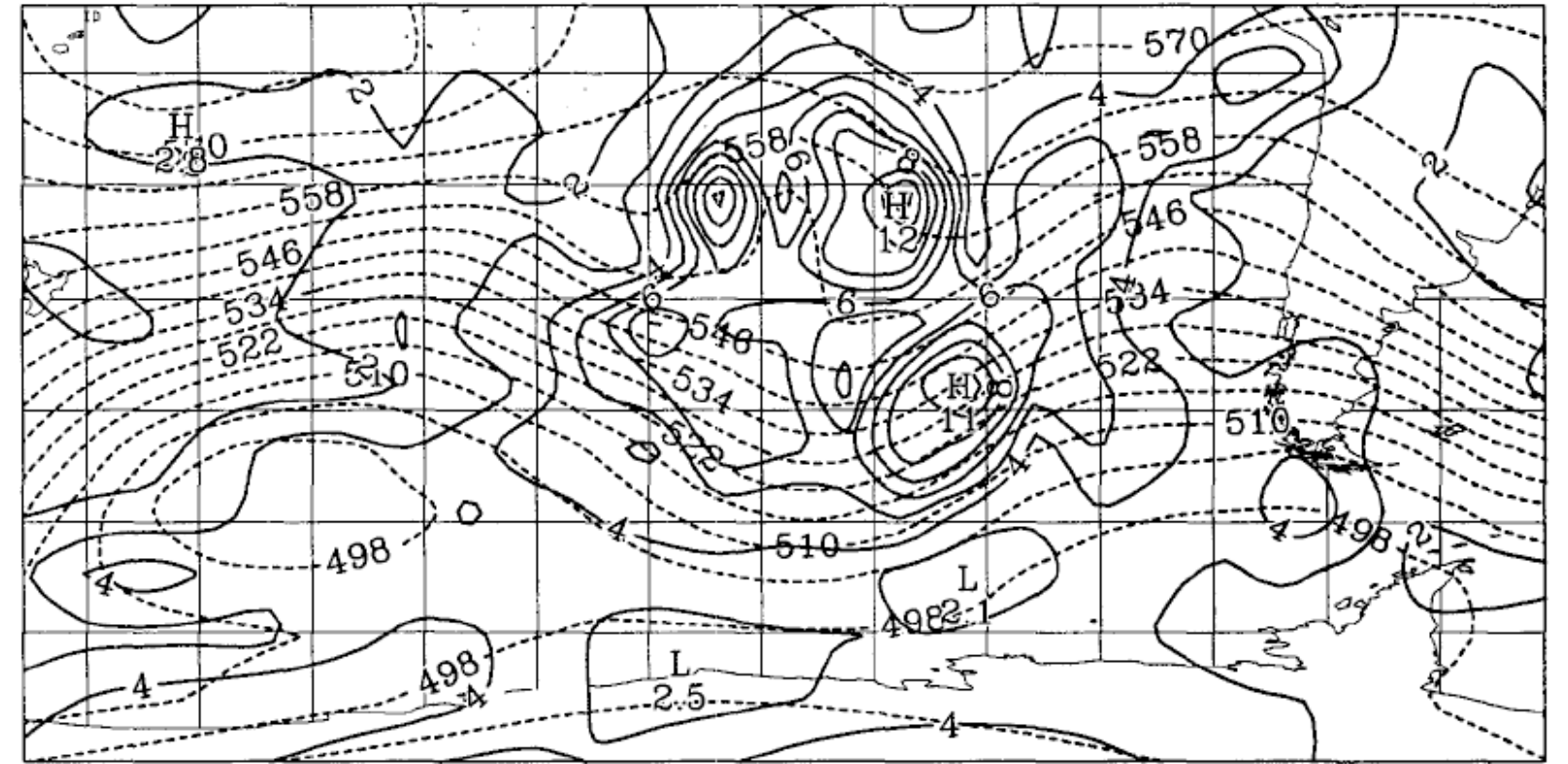
T = 24 (HRS)
ANALYSIS ERROR VARIANCE (500 MB)



T = 24 (HRS)

FIG. 5. Analysis error variance at the final time for an assimilation without the time integration of the forecast error covariances. A contour interval of $0.5 \times 10^{-12} \text{ s}^{-2}$ has been used.

B) ERROR VARIANCE AND GEOPOTENTIAL



T = 24 (HRS)

FIG. 4. Analysis error variance field at $t = 24 \text{ h}$ superposed over (a) the vorticity field and (b) the geopotential field. The domain is a close-up of the region west of South America.

Gauthier et al (1993)

Analysis error without time dependent forecast error covariance

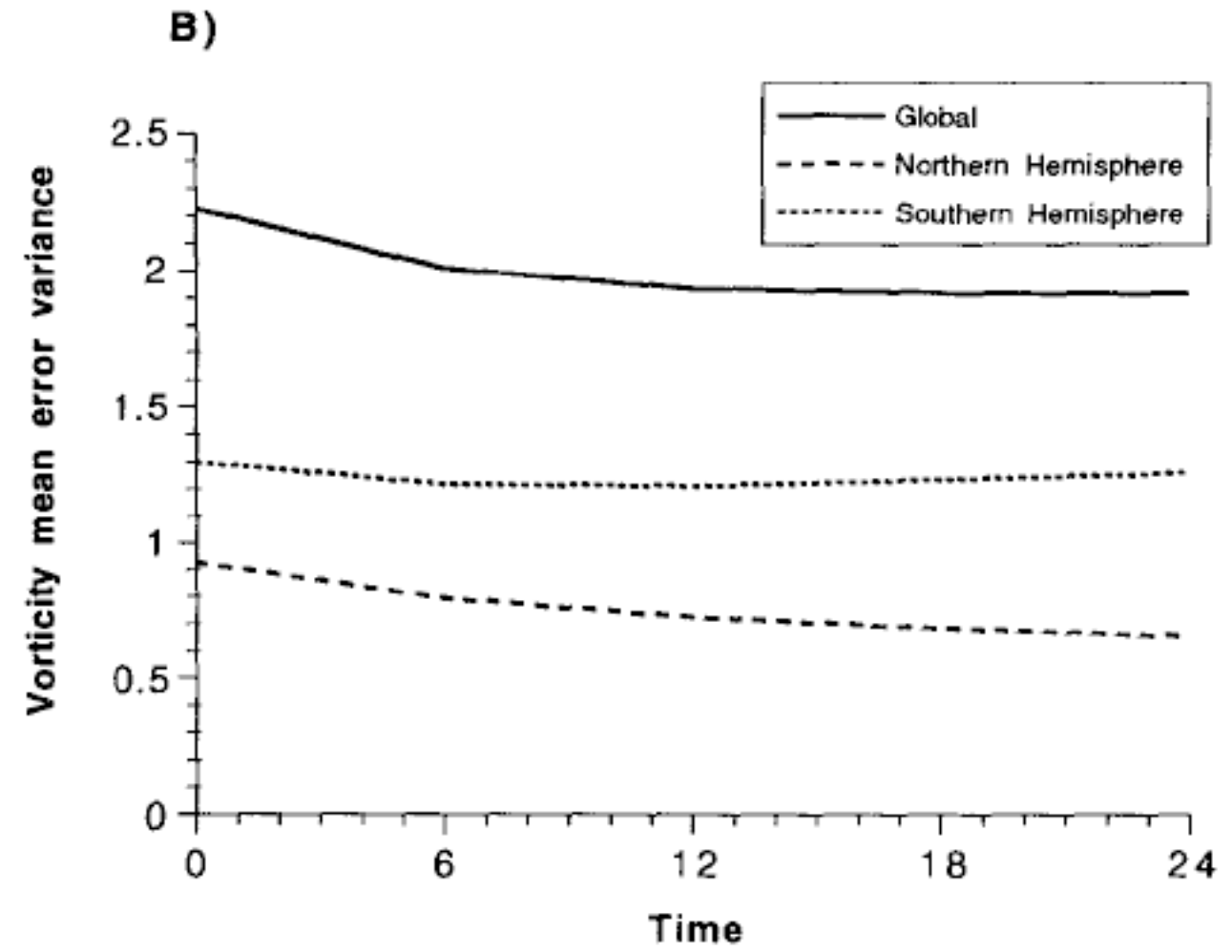
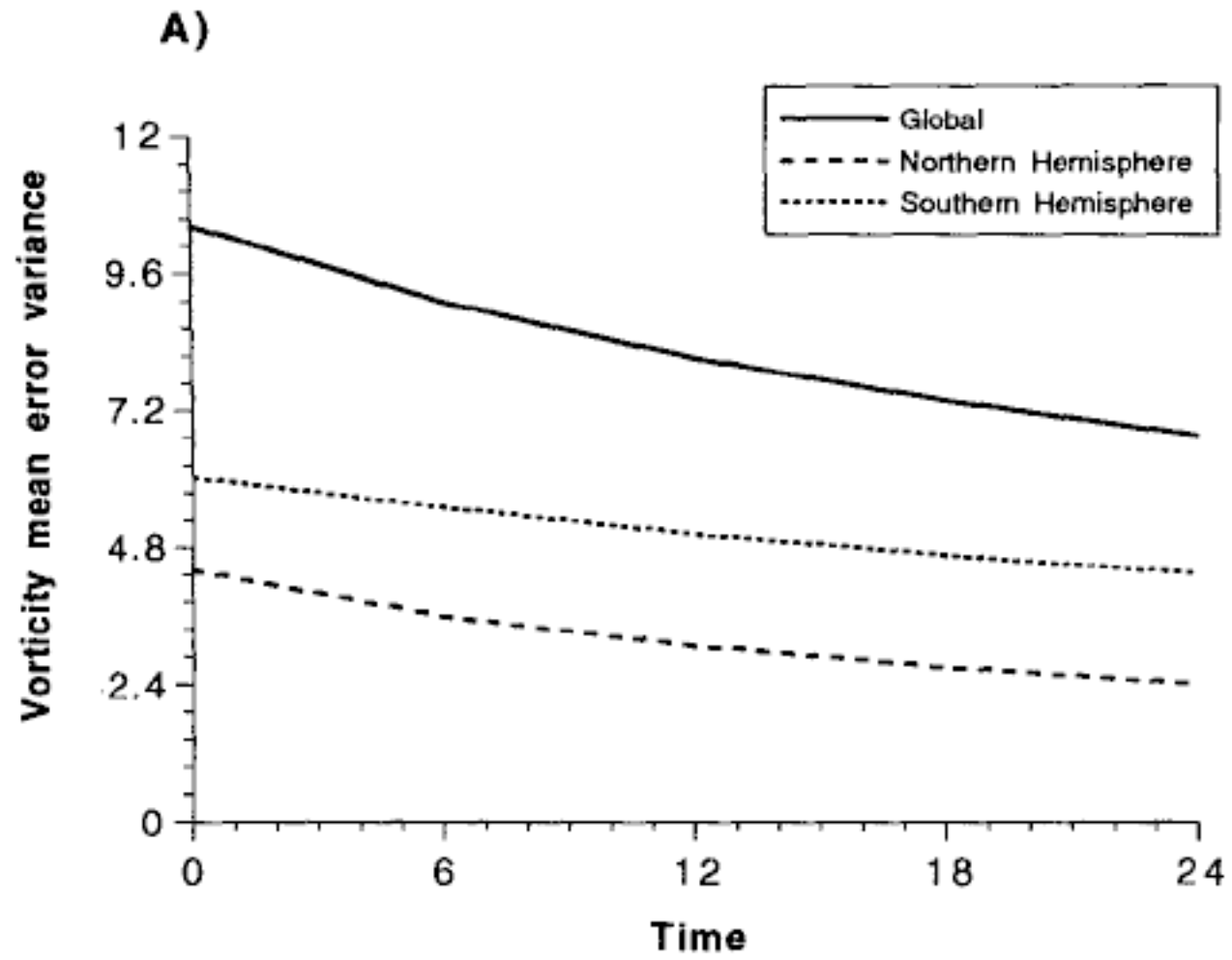
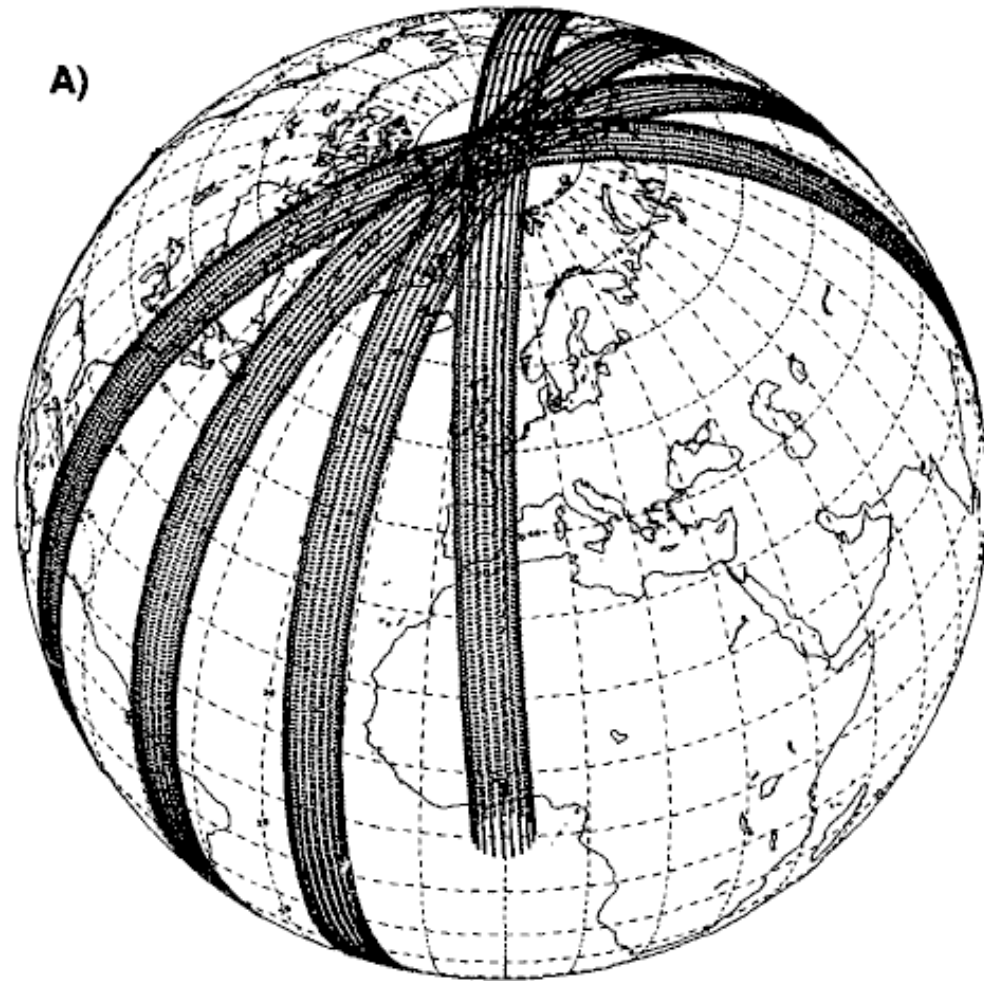


FIG. 7. Time evolution of the global mean analysis error variance (solid line) for a characteristic length of the first-guess error of (a) 400 km and (b) 1200 km. In both figures, the contributions from the Northern and Southern hemispheres have been plotted separately to emphasize the differences existing between the two hemispheres.

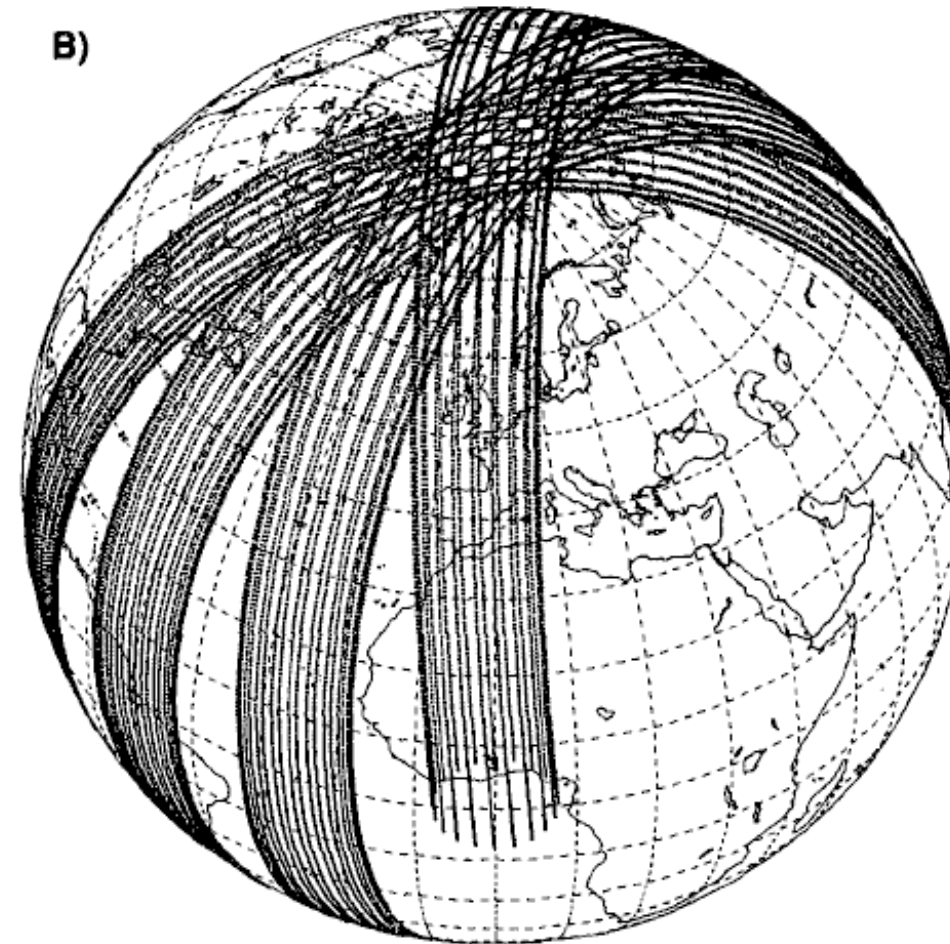
Pseudo data from Space

400 km Orbit



Observation error: 1 m/s

800 km Orbit



Observation error: 4.3 m/s

FIG. 8. Typical data coverage for a satellite on a polar orbit at an altitude of (a) 400 km and (b) 800 km. Distribution of the points corresponds to those of a conical scan with a scanning period of 10 s. The shot frequency was set to 2 Hz.

400 km Orbit

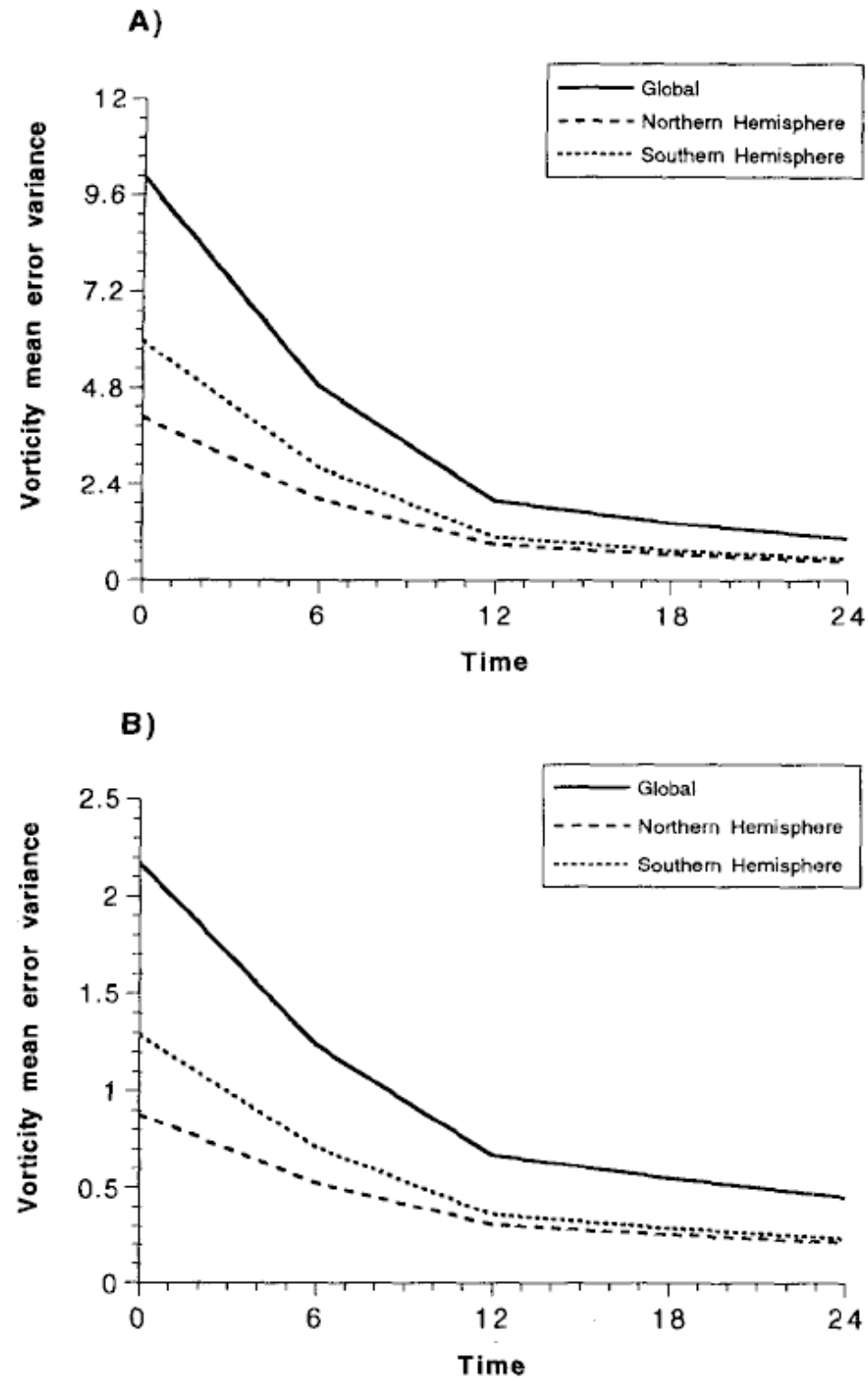


FIG. 9. As in Fig. 7 but for an assimilation using the Lidar data coming from a satellite on a polar orbit at an altitude of 400 km. Results are shown for two experiments using a characteristic length of the first-guess error of (a) 400 km and (b) 1200 km.

800 km Orbit

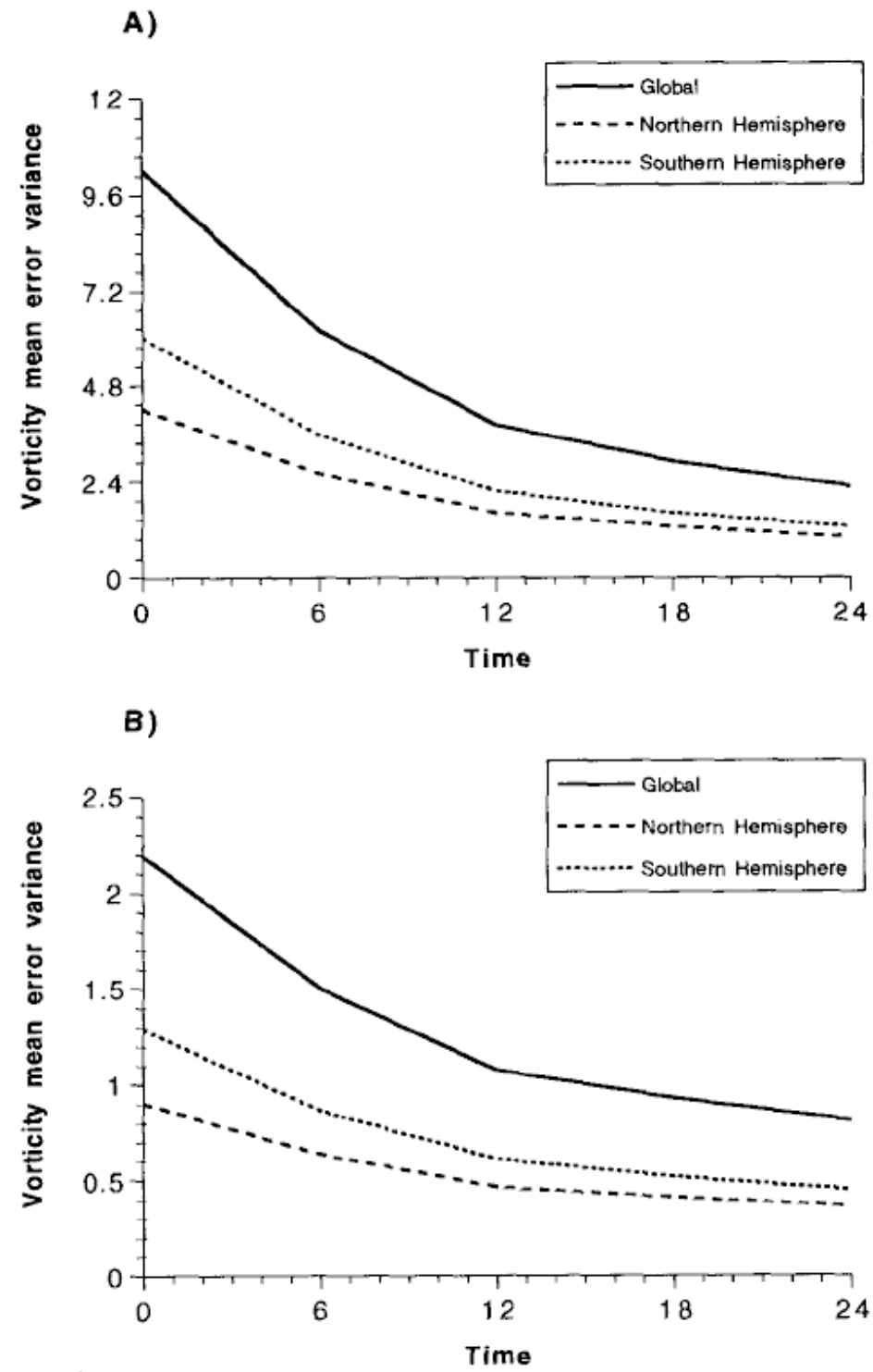
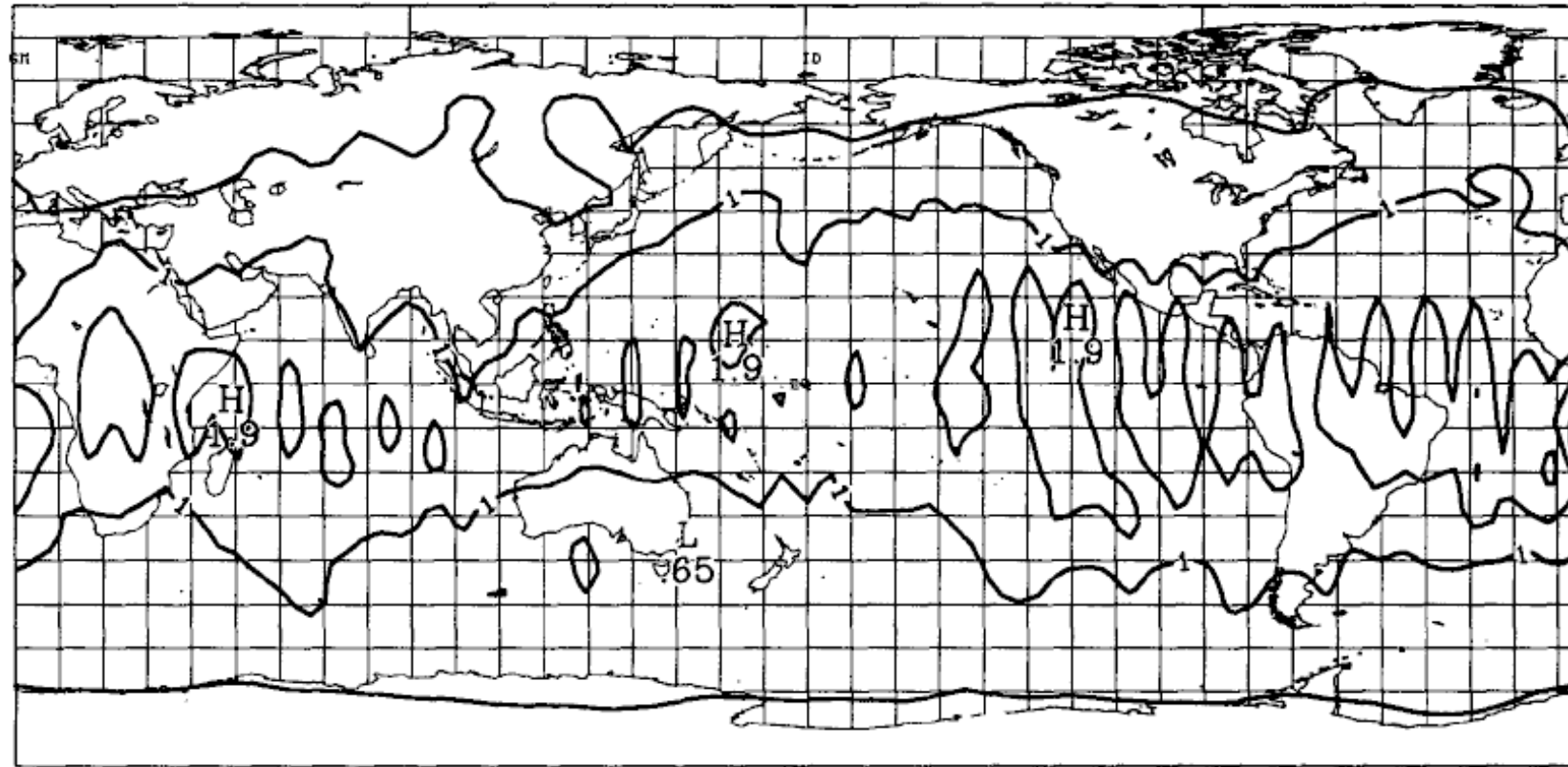


FIG. 10. Same as Fig. 9 but for a satellite at an altitude of 800 km.

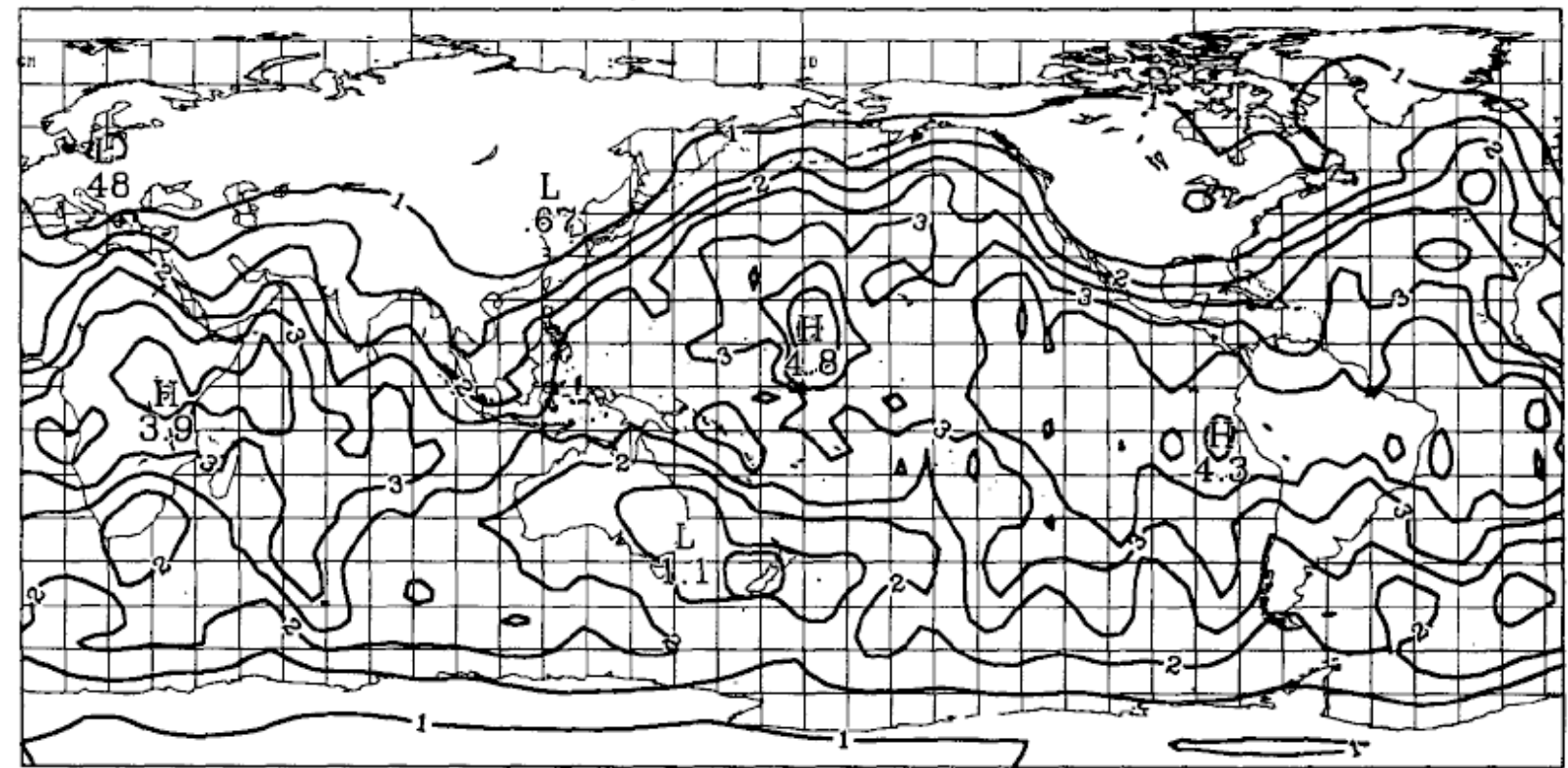
Analysis error for Lidar data

A) ALT.: 400 KM



T = 24 (HRS)
-C-

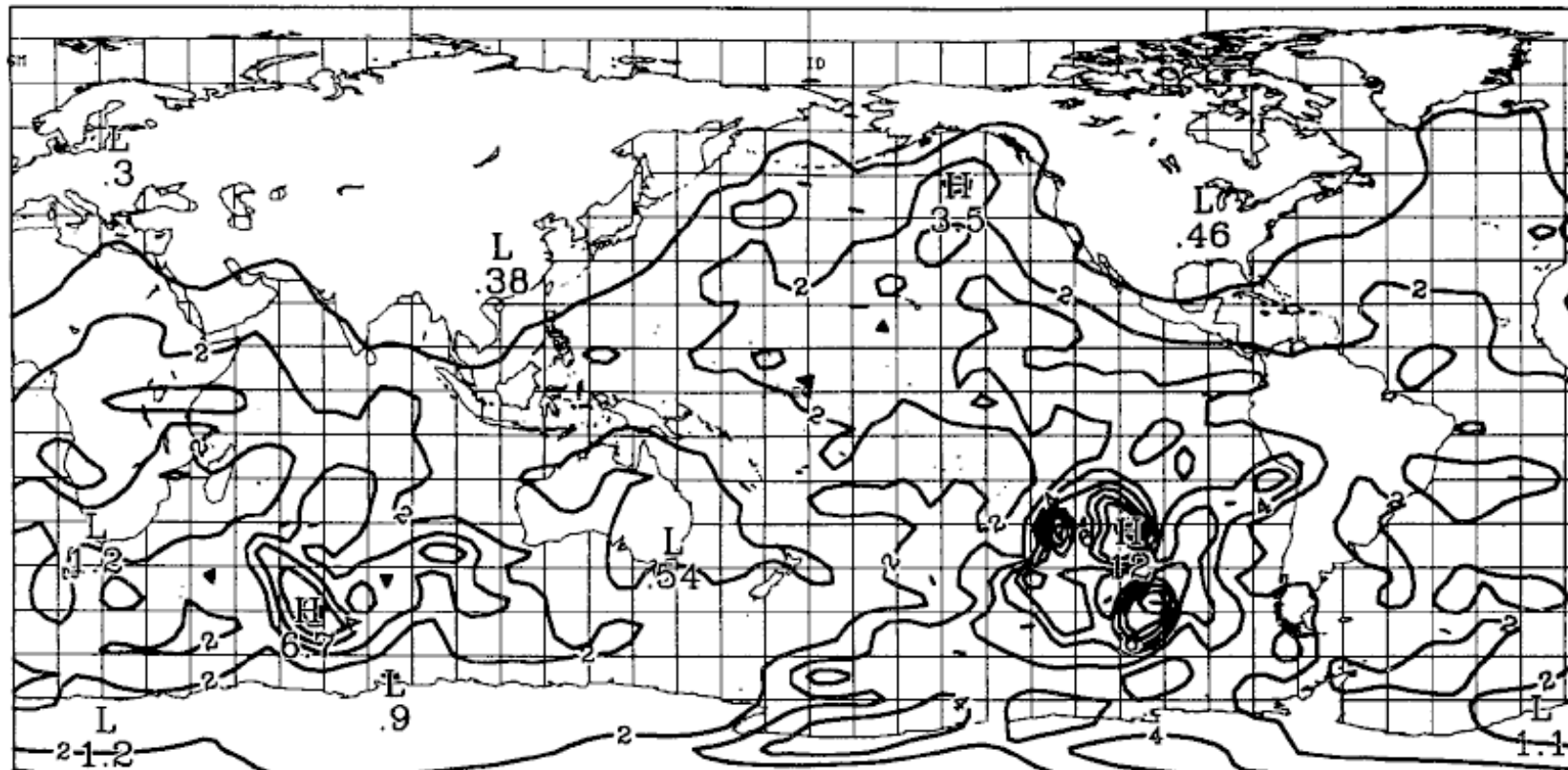
B) ALT.: 800 KM



T = 24 (HRS)

FIG. 11. Analysis error variance field at $t = 24$ h for an assimilation using Lidar data obtained from a satellite at an altitude of (a) 400 km and (b) 800 km. In both cases, a characteristic length of the first-guess error of 400 km has been used. A contour interval of $0.5 \times 10^{-12} \text{ s}^{-2}$ has been used.

Gauthier et al (1993)



T = 24 (HRS)

Analysis error for in situ network

A simple example

Evensen (1992)

Model: 1-D linear advection equation in a periodic domain:

$$\frac{\partial F}{\partial t} + c \frac{\partial F}{\partial x} = 0$$

- Truth = sinusoid traveling left to right
- perfect obs at $x=5$ and $x=20$, every 5 time steps. Error variance $2\times$ worse at $x=20$.
- background is $F = 0$
- background error variance is 1, correlation function $\sim \exp[-(r/r_c)^2]$

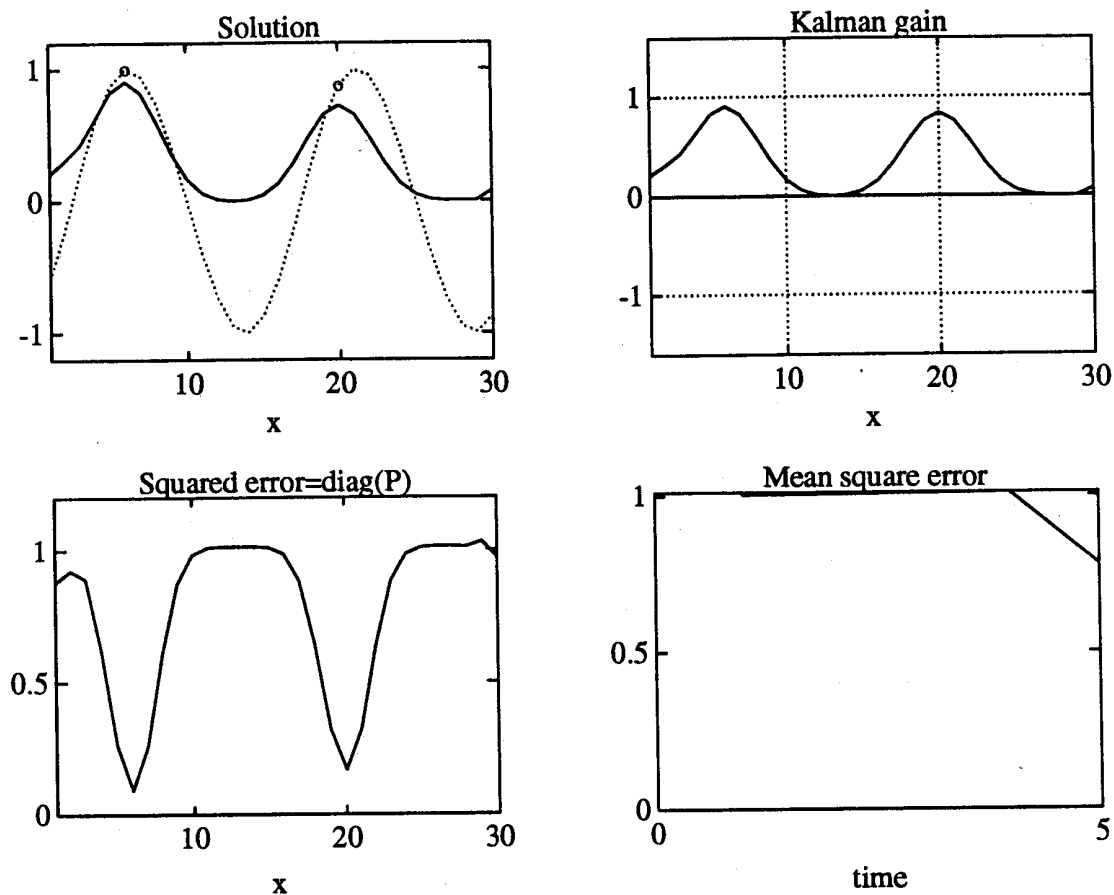


Fig. 1. Solution of the advection equation after one update with the Kalman filter. The upper left plot shows the true solution as a dotted line and the estimated solution as the solid line. The circles are the values of the measurements. The lower left plot shows the estimated error variance for each grid point (the diagonal elements of P). The Kalman gain influence (columns of K) are shown in the upper right plot. The lower right plot shows the time history of the mean square error, i.e., the normalized trace of P .

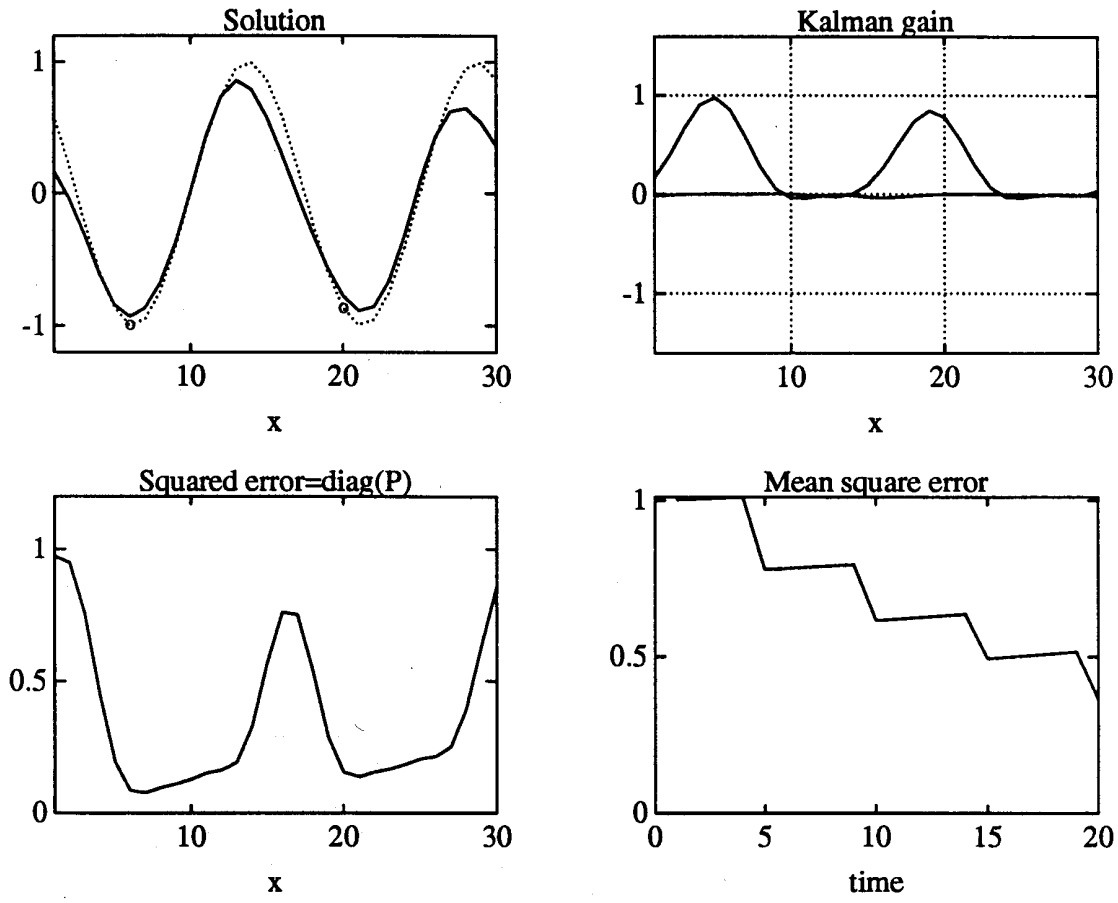


Fig. 2. The same as Figure 1 but after four updates with the Kalman filter.

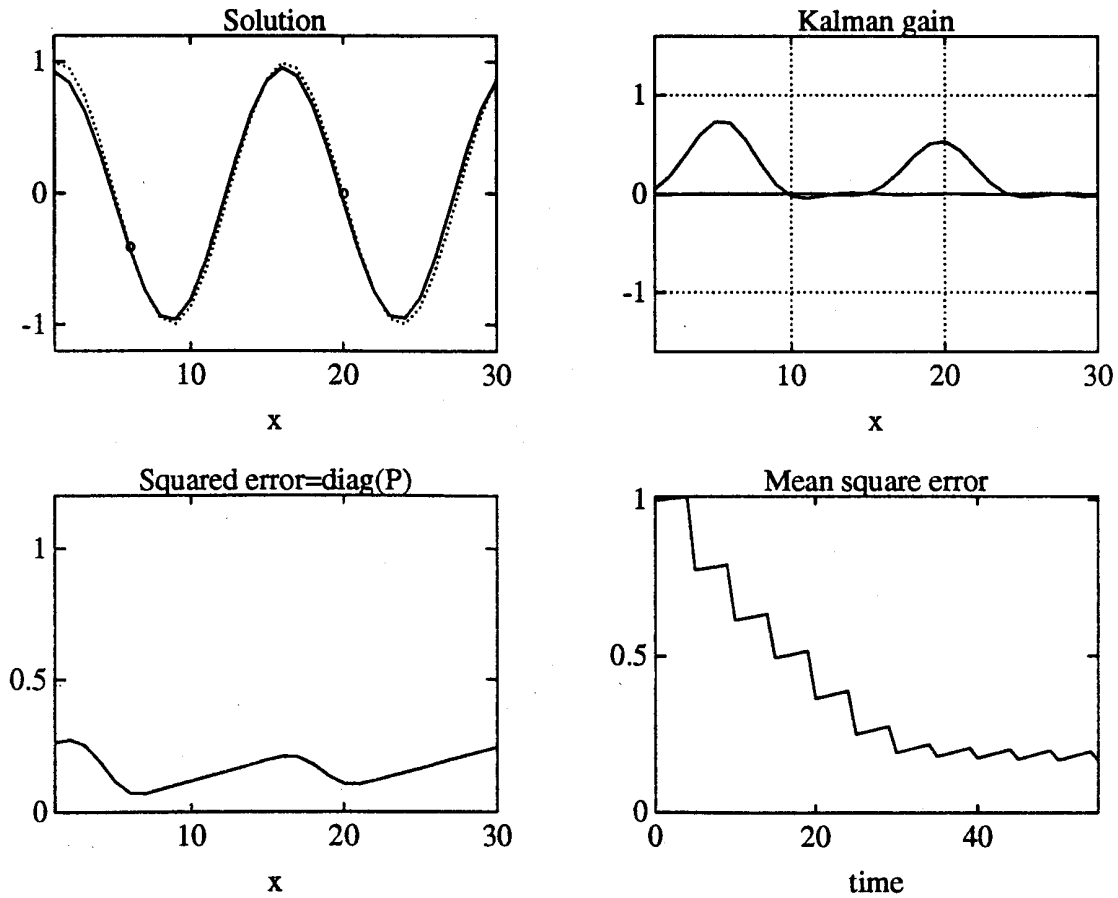


Fig. 3. The same as Figure 1 but after 11 updates with the Kalman filter.

Evensen (1992)